4 Ultraviolet Radiation and the Optical Properties of Sea Ice and Snow

D.K. PEROVICH

4.1 Introduction

The continuing annual appearance of ozone holes in the Arctic and Antarctic results in recurring periods of enhanced incident ultraviolet irradiance at the earth's surface. Indeed, a recent analysis of incident ultraviolet irradiance measured at Barrow, Alaska, from 1991 to 1995 demonstrates a continuing increase in ultraviolet light levels (Gurney 1998). Much of the area most affected by stratospheric ozone depletion is covered by a seasonal or perennial sea-ice cover, which is a productive ecological habitat. To determine the impact of enhanced incident ultraviolet irradiance on this habitat, an understanding of the interaction of ultraviolet light with snow and sea ice is required.

It is well established that ultraviolet irradiance can have a deleterious effect on primary productivity in the open ocean and in marginal ice zones (Smith et al. 1992; Prezelin et al. 1994, 1998). Damage has also been found in under-ice communities (Prezelin et al. 1998), indicating that pack ice does not provide complete protection from ultraviolet light. Antarctic studies have established that marine particulates (Vernet et al. 1994), algae (Karentz 1994), phytoplankton (Heibling et al. 1994), DNA, protein, and the amino acid porphyra-334 (Prezelin et al. 1998) strongly absorb ultraviolet light.

Determining the biological impact of ultraviolet light in regions covered by sea ice is complicated by the temporal and spatial variability of the ice cover, in both its morphology and its optical properties. At ultraviolet and visible wavelengths, sea ice is a highly scattering, translucent medium. Scattering depends on the morphological structure of the ice and on the surface conditions. For most of the year, from September through June, the sea ice is covered by snow. This chapter focuses on the interaction of ultraviolet light with sea ice and snow. A brief description is given of sea-ice morphology followed by a synopsis of radiative transfer theory as applied to sea ice. A summary of results from observational and modeling studies is then presented.

Ecological Studies, Vol. 153
D. Hessen (ed.) UV Radiation and Arctic Ecosystems

4.2 Sea-Ice Structure and Morphology

The optical properties of sea ice are intimately related to its physical state and structure (Grenfell and Maykut 1977; Perovich 1996). Physical changes in the ice or snow cover result in changes in the reflection and transmission of the incident ultraviolet irradiance. The sea-ice cover exhibits tremendous spatial variability: over distances of only tens of meters, conditions can range from

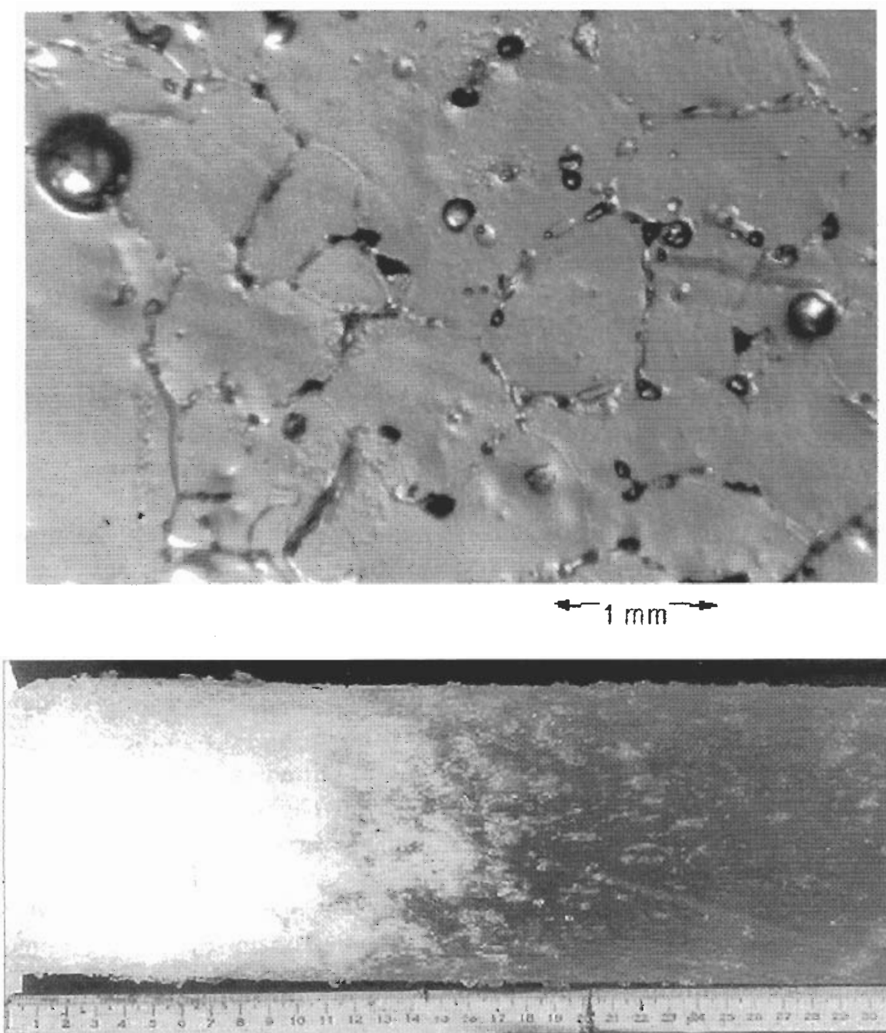

Fig. 4.1. The small-scale structure of sea ice: **a** ice core of upper portion of multiyear ice and **b** photomicrograph of horizontal thin section of sea ice showing brine pockets and air bubbles

open water to young ice only a few centimeters thick to pressure ridges tens of meters thick. Snow depths can vary from bare ice to drifts more than a meter deep. In summer, areas of ponded meltwater are also present.

There is also spatial variability on the small scale. Sea ice is a material that exists at its salinity-determined melting point, so changes in temperature result in changes in the physical properties and structure of the ice. Sea ice has an intricate microstructure consisting of an ice matrix with inclusions of air bubbles, brine pockets, and solid salts. Impurities, such as particulates and biogenic material, may also be present. The photomicrograph in Fig. 4.1a illustrates the small-scale structure of sea ice. The larger, rounded features are

Fig. 4.2. Arctic pack ice in **a** spring and **b** summer. In spring, the surface is covered with snow and has a uniform appearance; by summer, it has evolved into a mixture of bare ice, ponded ice, and leads

air bubbles, and the smaller elongated elements are brine pockets. As we shall see, these inclusions are the primary scatterers of light in sea ice, and scattering dominates ultraviolet radiative transfer in sea ice.

Sea ice also changes temporally. It undergoes a major morphological evolution during the summer melt season, as Fig. 4.2 illustrates. In spring (Fig. 4.2a), when ozone depletion is at the maximum, over 90% of the ice is covered by an optically thick layer of snow (>0.1 m), and average spring snow depths are about 0.35 to 0.4 m (Warren et al. 1999; Sturm et al. 2001). The snow cover gives the ice a uniform appearance and a high albedo. The albedo can reach values as high as 0.98 at visible wavelengths (Grenfell et al. 1994). In spring, this high surface albedo not only affects the reflected and transmitted ultraviolet irradiance, but the incident irradiance as well. The presence of a snow cover causes an increase in incident ultraviolet irradiance at the surface due to multiple reflections between the sky and the surface (McKenzie et al. 1998). Typically, in early June the snow begins to melt, ultimately transforming this once uniform surface into a variegated mosaic of bare ice, melt ponds, and open water (Fig. 4.2b). Associated with these melt-induced morphological changes is an overall decrease in the albedo and an increase in the transmittance.

Understanding the many and varied nuances of sea-ice morphology is a daunting task. Fortunately, there are several excellent overview articles describing the large-scale and small-scale properties of the polar ice covers (Weeks and Ackley 1982; Gow and Tucker 1990; Tucker et al. 1993; Weeks 1998).

4.3 Theory

Radiative transfer theory is well developed for atmospheres, oceans, and ice covers. The discussion here is limited to a general description of radiative transfer processes. For models focusing on sea ice and snow, a plane parallel medium is usually assumed, that is, a medium that is horizontally infinite and horizontally homogeneous, but with vertically varying properties. The formal equation of radiative transfer for a plane parallel medium is (Chandrasekhar 1960)

$$-\mu \frac{dI(\tau,\mu,\phi,\lambda)}{d\tau} = I(\tau,\mu,\phi,\lambda) - S(\tau,\mu,\phi,\lambda) \tag{4.1}$$

where I is the radiance, λ is the wavelength, μ is the cosine of the zenith angle (θ), and ϕ is the azimuth angle. τ is the nondimensional optical depth and is defined as

$$\tau(\lambda)=(k(\lambda)+\sigma(\lambda))z \tag{4.2}$$

where k is the absorption coefficient, σ is the scattering coefficient, and z is the physical depth. In Eq. (4.1), the effects of scattering are treated in the S term, which is referred to as the source function and defined as

$$S(\tau,\mu,\phi,\lambda)=\frac{\varpi_o}{4\pi}\int_{-1}^{1}\int_{0}^{2\pi}p(\mu,\mu',\phi,\phi')I(\tau,\mu',\phi',\lambda)d\mu'd\phi-\frac{E_O(\lambda)}{4}e^{-\tau(\lambda)/\mu_o}, \tag{4.3}$$

where $p(\mu,\mu',\phi,\phi')$ is the phase function and E_0 is the radiance of the direct beam component of the incident radiation field. The double integral term represents scattering of the diffuse radiance field $I(\tau,\mu',\phi',\lambda)$. The second term provides the contribution of scattered light from the attenuated direct beam $[E_0(\lambda)]$. The phase function (p) defines how much light is scattered from one direction (μ,ϕ) to another (μ',ϕ'). For the mathematical details of, and solutions to, the integro-differential equation of radiative transfer, readers are directed to several excellent volumes including Chandrasekhar (1960), Liou (1974), Bohren and Huffman (1983), and Mobley (1994). For the purposes of this chapter, the key point is that radiative transfer in snow and ice is governed by two processes, absorption and scattering. Absorption is characterized by the absorption coefficient (k), which is a measure of the amount of absorption per unit length. For scattering, the key parameters are the scattering coefficient (σ), which is a measure of the amount of scattering, and the phase function (p), which describes the angular distribution of scattered light.

The Arctic snow pack is primarily a mixture of ice, air, and, during melt, water. Sea ice consists of ice, brine, and air. Absorption of light in the air contained in sea ice and snow is assumed to be negligible. Ultraviolet absorption coefficients for pure bubble-free ice (k_i; Grenfell and Perovich 1981; Perovich and Govoni 1991) and water (k_b; Smith and Baker 1981) are plotted in Fig. 4.3. Visible values are also plotted for comparison. In the ultraviolet, ice and water absorption coefficients increase as wavelength decreases. Absorption coefficients for the ice and water are similar in shape and magnitude. These values provide the building blocks for determining absorption coefficients in sea ice (k_{si}), which can be calculated by weighting the absorption coefficients by the relative volumes of ice (v_i) and brine (v_b; Grenfell 1983):

$$k_{si}=\nu_i k_i+\nu_b k_b. \tag{4.4}$$

For cold, multiyear ice, brine volume is small and $k_{si}\sim k_i$. Both snow and sea ice often contain impurities such as dust, soot, and biogenic material. These impurities are usually strongly absorbing and weakly scattering; if they are present in sufficient quantity, their absorptive properties should also be

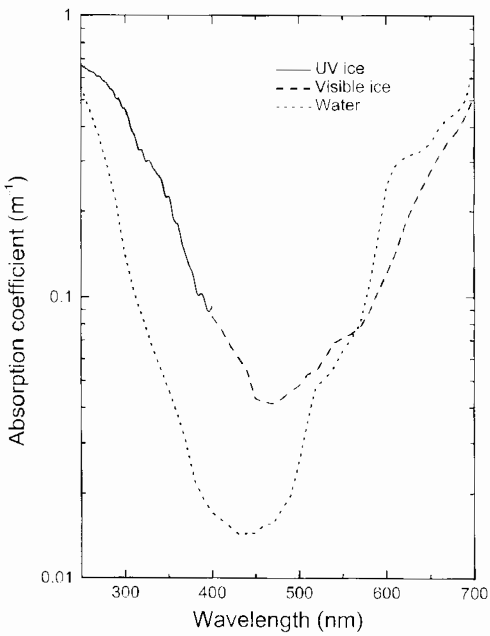

Fig. 4.3. Absorption coefficient of ice and water from the UV through the visible for pure bubble-free ice (Grenfell and Perovich 1981; Perovich and Govoni 1991) and water (Smith and Baker 1981)

included in radiative transfer calculations. At ultraviolet wavelengths, this is particularly true for biogenic materials.

Scattering in sea ice results from differences in the real indices of refraction (n) between ice (n~1.31) and the inclusions. Sea ice has a large number of brine pockets (n~1.33–1.36) and air bubbles (n~1), and is therefore a highly scattering medium. Scattering coefficients and phase functions are difficult to measure in a highly scattering medium like sea ice. Indeed, there are very few such measurements (Grenfell and Hedrick 1983), and none were made at ultraviolet wavelengths. In addition, because scattering is determined by the highly variable structure of sea ice, scattering coefficients are also highly variable.

The larger the difference in index of refraction, the greater the amount of scattering. Hence, air bubbles scatter more strongly than brine pockets. If the ice is cold enough that solid salts form, scattering increases significantly, since these salts are very effective scatterers (Perovich and Grenfell 1981). Sea-ice scattering coefficients depend not only on the amount of brine and air, but on how they are distributed. More inclusions in the ice result in more scattering and, consequently, a larger scattering coefficient. For example, the upper portion of the ice core in Fig. 4.1b has many more air bubbles and more scattering than the lower portion, as is evident in the photograph. Sea ice scattering coefficients determined at visible wavelengths are large, with values typically greater than 10/m for warm ice and greater than 200/m for drained bubbly ice (Perovich and Grenfell 1982; Grenfell 1983, 1991; Grenfell and

Hedrick 1983). Both observations (Grenfell and Hedrick 1983) and theoretical calculations (Maykut and Light 1995) indicate that sea ice is strongly forward scattering, with the phase function decreasing by three to five orders of magnitude from forward to backward scattering.

Since the scatterers are much bigger than ultraviolet and visible wavelengths and the real portion of the index of refraction for ice and brine is fairly constant with wavelength, a major simplification can be made: scattering coefficients and phase functions are assumed to be constant with wavelength (van de Hulst 1981; Bohren and Huffman 1983; Grenfell 1983, 1991; Perovich 1993). A similar argument is applied to scattering in snow (Bohren and Barkstrom 1974; Wiscombe and Warren 1980). This implies that ultraviolet scattering coefficients are approximately equal to visible values, and the relatively large database on scattering in sea ice and snow at visible wavelengths can be used as a first-order proxy for the ultraviolet properties. There has been much more work, both observationally and theoretically, on the optical properties of sea ice at visible wavelengths than at ultraviolet wavelengths (Maykut and Grenfell 1975; Grenfell and Maykut 1977; Grenfell 1979, 1983, 1991; Grenfell and Perovich 1981; Perovich and Grenfell 1981, 1982; Warren 1982; Trodahl et al. 1987; Perovich 1990; Arrigo et al. 1991, 1993; Jin et al. 1994; Mobley et al. 1997; Perovich et al. 1998a,b).

The key theoretical points regarding the radiative transfer in sea ice are that (1) absorption coefficients for ice, brine, and impurities depend strongly on wavelength; (2) the scattering coefficients and phase functions for sea ice are constant with wavelength, allowing results from visible wavelengths to be used in the ultraviolet; (3) air bubbles scatter more strongly than brine pockets, and (4) increasing the number of inclusions in sea ice increases the amount of scattering.

4.4 Observations

While absorption and scattering coefficients are fundamental properties of snow and sea ice, they are often difficult to measure and not of prime interest for biological studies. Determining the distribution of the incident ultraviolet irradiance between reflection from the surface, absorption in the snow and ice, and transmittance to the ocean is often the objective. The most studied optical property of sea ice or snow is the albedo (α). Albedo is simply defined as the fraction of the incident irradiance that is reflected. Sea ice albedos in the ultraviolet range, like visible albedos, are sensitive to surface conditions. For example, the presence of a snow cover causes an increase in albedo, while surface water elicits a decrease. Ultraviolet albedos for three snow cases and three sea ice cases are plotted in Fig. 4.4.

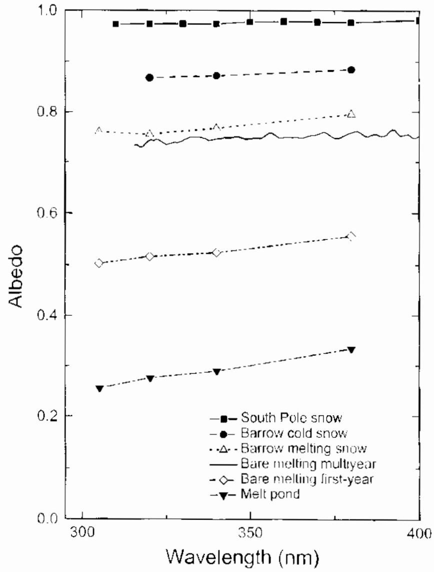

Fig. 4.4. Observations of spectral albedos for snow and sea ice. (Grenfell et al. 1994; Perovich 1995, 1998a,b)

Snow has a multitude of small grains and ice/air interfaces and is a highly scattering medium with a large albedo. The presence of particulates in the snow, such as dust or soot, reduce the albedo. The albedos for the exceptionally clean snow at the South Pole are quite large (0.98) and uniform across the spectrum (Grenfell et al. 1994). The albedo of cold, dry snow over shorefast sea ice at Barrow, Alaska, is also plotted in Fig. 4.4. These albedos are markedly smaller (0.9) than the South Pole results. The difference results from the large amount of particulates present in the Barrow snow pack. These curves effectively bound the range of ultraviolet albedos found for cold, dry snow. Because snow is highly scattering, it only takes a relatively thin 10- to 15-cm layer of snow to produce these large albedos. When snow melts, some of the ice/air interfaces become ice/water interfaces, and there is a reduction in scattering and a decrease in the albedo to 0.75–0.8 (Quakenbush and Wendler 1994; Perovich et al. 1998a,b).

Albedos for bare, melting multiyear ice are similar to melting snow values (Grenfell, pers. comm.). During melt, multiyear sea ice in the Arctic typically has a surface granular layer that is 1–3 cm thick, similar to coarse-grained snow, which is highly scattering (Perovich et al. 2001). Because of this layer, albedos range between 0.7 and 0.8. Melting first-year ice typically does not develop such a pronounced surface scattering layer and consequently has smaller albedos (0.5–0.55). Meltwater accumulates on the surface in some areas of the ice cover, forming melt ponds. The surface water is a layer where there is absorption but very little scattering. Consequently, pond albedos are less than bare-ice albedos. They are also variable, depending in large part on the physical properties of the underlying ice and to a lesser extent on the depth of the pond. Ultraviolet pond albedos are wavelength-dependent, decreasing from 400 to 300 nm (Fig. 4.4).

The amount of light transmitted through an ice cover is a key quantity when assessing the impact of ultraviolet light on biota living in or under a sea ice cover. The transmittance (*T*) is the fraction of the incident irradiance that is transmitted through the ice. Like the albedo, transmittance is sensitive to surface conditions. It also depends on the physical composition of the ice and is a strong function of the thickness of the ice. Indeed, the transmittance drops off roughly exponentially with increasing ice thickness. While not as numerous as albedo observations, ultraviolet transmittance measurements have been made through snow and sea ice (Trodahl and Buckley 1990; Wendler and Quakenbush 1993; Perovich 1995; Perovich et al. 1998a,b).

Perovich et al. (1998a) examined ultraviolet and visible albedo and transmittance for a typical spring-summer evolutionary sequence of first-year ice (Fig. 4.5). The sequence was (1) cold ice covered by 0.1 m of cold snow, (2) ice with 0.06 m of melting snow, (3) bare melting ice, and (4) a 0.1-m-deep melt pond. The ice thickness was roughly 1.6 m. The albedo, at all wavelengths, decreased throughout this melt sequence (Fig. 4.5a). The decrease

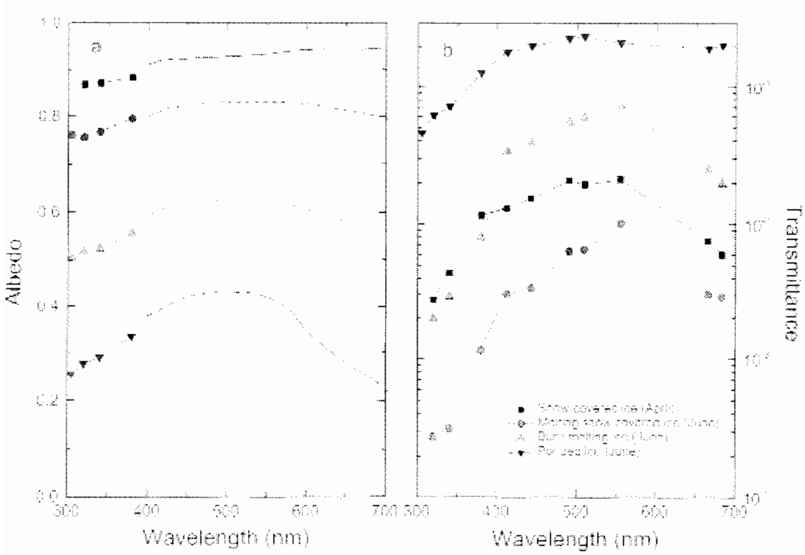

Fig. 4.5. The evolution of **a** albedo and **b** transmittance during the onset of melt (from Perovich et al. 1998a,b). The *curves* represent a typical evolutionary sequence for first-year ice from April through June: 0.1 m of cold snow over ice, 0.6 m of melting snow over ice, bare melting ice, and a 0.1-m-deep melt pond. The ice thickness was 1.6 m in all cases. The melting snow-covered ice and the bare-ice cases had significant amounts of ice biota present at the bottom of the ice

was greater in the ultraviolet than in the blue-green portion of the spectrum. Albedos at 305 nm decreased by more than a factor of three between the cold snow-covered ice (0.88) and the ponded ice (0.25).

Considering the optical properties of only the snow and ice, we would expect that spectral transmittance would evolve in a similar fashion, with the transmittance increasing as the albedo decreases. However, as Fig. 4.5b indicates, this was not the case. Contrary to our simple notions, as the snow began to melt, the transmittance decreased at all wavelengths due to a 20-fold increase in the algal biomass present in the skeletal layer at the bottom of the ice. Perovich et al. (1998a,b) state that the enhanced ultraviolet absorption and shift in maximum transmission to longer wavelengths is consistent with absorption in an algal layer (Maykut and Grenfell 1975; Arrigo et al. 1991; Fritsen et al. 1992; Zeebe et al. 1996). During the transition from snow-covered to bare ice, much of the algae sloughed off the bottom, decreasing the biomass by an order of magnitude, but enough remained to noticeably impact ultraviolet transmission. Ultraviolet transmittance was greatest for the ponded case ranging from 0.05 to 0.10, when the amount of biomass was at a minimum. The key point is that biogenic materials can greatly impact the transmission of ultraviolet light through sea ice.

4.5 Models

The extreme spatial and temporal variability of the physical and optical properties of sea ice, and the difficulties involved with measuring light transmission through sea ice, make models essential in interpreting and extrapolating observations. For example, models can be a primary tool for studies of how the optical properties of a region evolve with time.

Because of this importance, there are several sea-ice radiative transfer models at visible and near-infrared wavelengths. There are discrete ordinate solutions (Chandrasekhar 1960) using two streams (Grenfell 1979; Perovich 1993), four streams (Perovich and Grenfell 1982; Grenfell 1991), 16 streams (Grenfell 1983), and a generalized *n* streams (Mobley et al. 1997) for radiative transfer in the snow and ice. There are Monte Carlo models (Trodahl et al. 1987) and exponential decay models, as well as models focused on sea ice bio-optics (Arrigo et al. 1991) and radiative transfer in the atmosphere-ice-ocean system (Jin et al. 1994).

While these models are for visible and near-infrared wavelengths, it is relatively straightforward to translate the models to ultraviolet wavelengths. As was stated in the theory section, scattering parameters are essentially the same in the ultraviolet range as the visible range. Absorption in the ice and brine are different in the ultraviolet than in the visible, so ultraviolet absorption coefficients for ice and brine from Fig. 4.3 are used. Absorption in any biogenic material may also be quite different in the ultraviolet (Fig. 4.5), so appropriate ultraviolet coefficients need to be used.

Perovich (1993) formulated a multilayer, two-stream, ultraviolet radiative transfer model and applied it to Antarctic sea ice. Scattering (σ) and extinction coefficients [$\kappa(\lambda)$] for different snow and ice conditions were determined from visible observations made by Grenfell and Maykut (1977). Perovich and Govoni (1991) commented on the fortuitous similarities between ultraviolet and visible absorption coefficients. For example, absorption coefficients at 720 and 250 nm are equal, as are values at 580 and 400 nm, allowing for mapping of visible and ultraviolet results. This correspondence, along with the wavelength independence of scattering, allows visible scattering and extinction coefficients to be mapped into the ultraviolet. Mapped extinction coefficients for relevant Arctic snow and ice types are plotted in Fig. 4.6 (Grenfell and Maykut 1977; Perovich 1993). Measured values for young ice and first-year ice that were determined directly from ultraviolet measurements (Perovich 1995) are also plotted for comparison. The measured extinction coefficients fall nicely within the range of the inferred values.

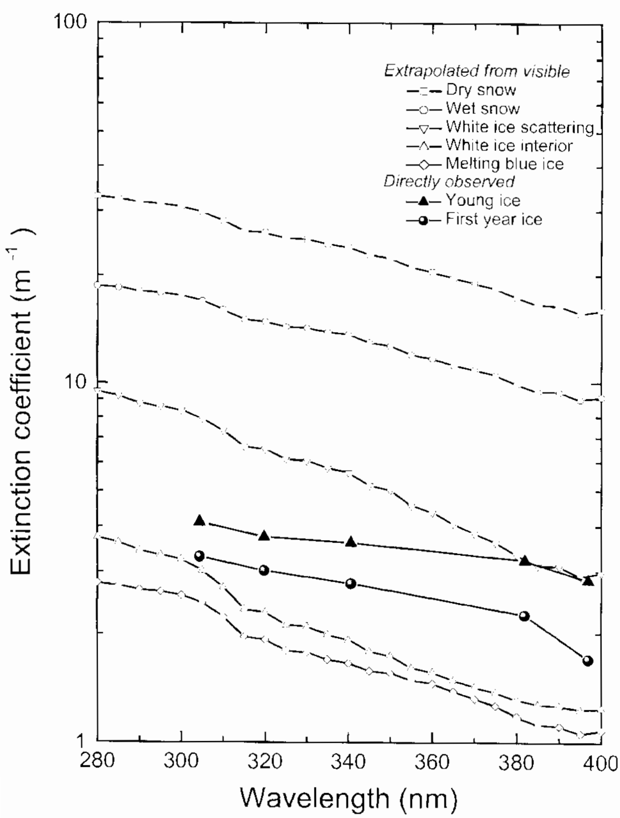

Fig. 4.6. Ultraviolet extinction coefficients mapped from visible values for snow and sea ice from Grenfell and Maykut (1977), along with measured values for young ice and first-year ice

The Antarctic simulations indicated that a sea ice cover significantly reduces the amount of ultraviolet light reaching the ocean and that snow is particularly effective at reducing ultraviolet transmittance. For example, a 10-cm-thick snow layer reduces UV-B by roughly two orders of magnitude. The attenuation of UV-B radiation by snow and ice was greater than UV-A radiation and photosynthetically active radiation (PAR). Thus, a sea ice cover may temper the biological impact of ultraviolet light by reducing the deleterious biological effective irradiance more than the beneficial photosynthetically active radiation.

There are differences in the physical and optical properties of Arctic and Antarctic sea ice (Weeks and Ackley 1982; Gow and Tucker 1990). In the Arctic, multiyear ice is predominant, the ice is thicker, and there is less flooded ice. Arctic multiyear ice is typically a few meters thick (Gow and Tucker 1990), and the average snow depth is roughly 40 cm (Warren et al. 1999; Sturm et al. 2001). Using the Perovich (1993) model, we will now investigate ultraviolet transmittance through Arctic sea ice. Isopleths of UV-B transmittance as a function of snow depth and ice thickness are plotted in Fig. 4.7. Moving from the origin of the plot toward deeper snow and thicker ice, each isopleth represents a decrease of an order of magnitude. For average values of snow depth (40 cm) and ice thickness (300 cm), transmitted ultraviolet irradiance is eight orders of magnitude less than the incident. The

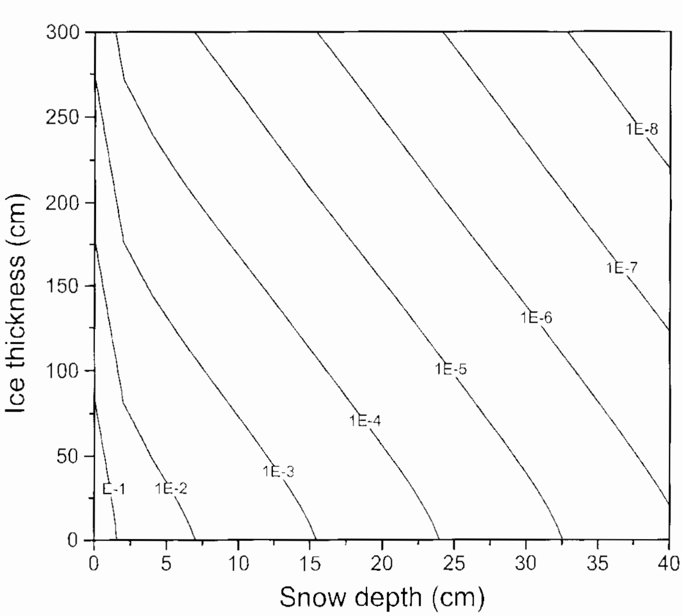

Fig. 4.7. Isopleths of UV-B as a function of snow depth and ice thickness for Arctic spring conditions

strong attenuation of ultraviolet light by snow is evident in the plot. An 8-cm snow layer causes approximately an order of magnitude reduction in ultraviolet irradiance.

Trodahl and Buckley (1989, 1990) and Buckley and Trodahl (1987) report that, for first-year Antarctic sea ice in McMurdo Sound, the period of the maximum ozone hole in spring coincides with maximum transmittance of the ice. They found that later in the season, as the ice began to melt, a drained surface scattering layer formed, reducing transmittance. As was mentioned earlier, a similar surface scattering layer is commonly observed to form during summer melt in the Arctic. However, unlike the Trodahl and Buckley (1989, 1990) Antarctic case, which had little snow, there is a substantial spring snow cover in the Arctic that has a considerable impact on transmittance.

The optical evolution of multiyear Arctic pack ice from spring through summer was investigated by applying the Perovich (1993) two-stream model. Two cases were considered: a melt pond and a hummock. Observations of snow depth, ice thickness, ice properties, and ice surface conditions made during the SHEBA field experiment for these two cases (Perovich 1999a,b) were used as input parameters to the model (Fig. 4.8a). Using these values and the two-stream model, time series of UV-B transmittances were calculated (Fig. 4.8b). The range of transmittance from spring to summer is striking,

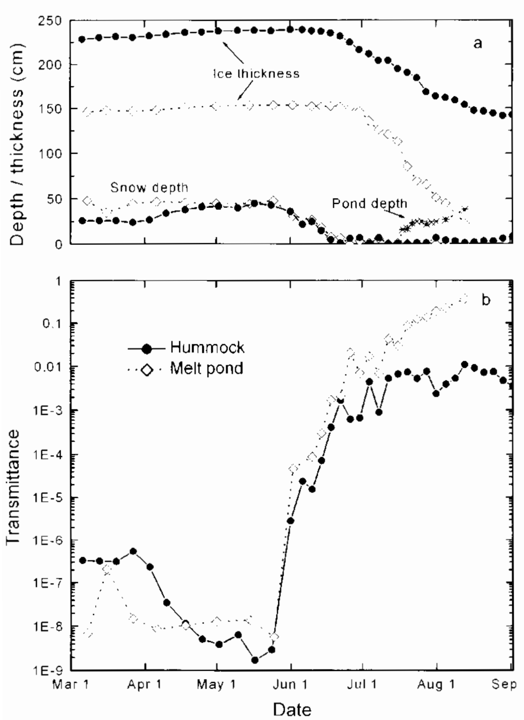

Fig. 4.8. a, b Evolution of UV-B transmittance from spring to summer melt for Arctic sea ice. Results for a hummock and a melt pond are plotted. Time series of snow depth, ice thickness, and pond depth obtained from field observations during SHEBA (Perovich et al. 1999b) were used as input parameters to the model

varying by more than eight orders of magnitude. In March, transmittance through the hummock was more than an order of magnitude greater than through the pond, even though the hummock was 75 cm thicker. Transmittance was less for the pond site because it was frozen and covered by 50 cm of snow, while the hummock had only 25 cm of snow. From the beginning of April to mid-May, transmittance at the hummock site decreased by a factor of 200 as the snow depth increased from 26 to 45 cm.

The major change in transmittance occurred in early June as the transmittance increased by six orders of magnitude in only a few weeks. This was a direct consequence of changes in the snow cover. When melt began in late May, the surface conditions abruptly shifted from dry snow to wet melting snow. For the next few weeks, snow depth decreased and the transmittance rapidly increased. By mid-June, the hummock and pond curves began to diverge. Transmittances for the hummock more or less stabilized between 0.001 and 0.01 as a surface scattering layer formed. Pond transmittances, however, continued to increase as the pond grew deeper and the ice thinner, reaching a value of 0.38 in mid-August. These large temporal changes demonstrate the importance of the timing of peak incident ultraviolet irradiance on potential biological impacts.

4.6 Summary

Sea ice and snow are highly scattering media. Scattering coefficients are large and approximately constant with wavelength. Absorption coefficients for pure ice vary with wavelength, increasing by a factor of 7 from 400 to 250 nm. There is considerable variability in the ultraviolet properties of snow and sea ice. Albedos are strongly dependent on surface conditions, with ultraviolet albedos ranging from more than 0.9 for snow to 0.7 for bare ice to 0.2 for ponded ice.

Transmittance depends on snow depth and ice thickness as well as surface conditions. In general, the presence of a sea ice cover, particularly one that is snow covered, dramatically reduces ultraviolet light reaching the ocean. For example, 10 cm of snow reduces UV-B transmittance by a factor of approximately 40. Sea ice and snow may provide protection for biota living in and under the ice, since attenuation is greater for deleterious UV-B than for beneficial PAR.

Although field observations and theoretical modeling results demonstrate that sea ice and snow greatly reduce ultraviolet irradiance, the biological consequences of this are far from evident. It is possible, for example, that ice biota may be shade-adapted with minimal defenses against UV-B and that even a small enhancement of ultraviolet transmittance could be harmful.

Interdisciplinary studies examining the impact of ultraviolet light on biological activity in and under the sea ice cover are needed to address this critical issue.

References

Arrigo KR, Sullivan CW, Kremer JN (1991) A bio-optical model of Antarctic sea ice. J Geophys Res 96:10581–10592

Arrigo KR, Kremer JN, Sullivan CW (1993) A simulated Antarctic fast ice ecosystem. J Geophys Res 98(C4):6929–6946

Bohren CF, Barkstrom BR (1974) Theory of the optical properties of snow. J Geophys Res 79(30):4527–4535

Bohren CF, Huffman DR (1983) Absorption and scattering of light by small particles. Wiley, New York, 530 pp

Buckley RG, Trodahl HJ (1987)Thermally driven changes in the optical properties of sea ice. Cold Regions Sci Technol 14:201–204

Chandrasekhar SC (1960) Radiative transfer. Dover, New York, 393 pp

Fritsen CH, Iturriaga R, Sullivan CW (1992) Influence of particulate matter on spectral irradiance fields and energy transfer in the eastern Arctic Ocean. Ocean Optics 11 Proc SPIE Int Soc Opt Eng 1750:527–541

Gow AJ, Tucker WB III (1990) Sea ice in the polar regions. In: Smith WO (ed) Polar oceanography, part A. Physical science. Academic Press, San Diego, pp 47–122

Grenfell TC (1979) The effects of ice thickness on the exchange of solar radiation over the polar oceans. J Glaciol 22:305–320

Grenfell TC (1983) A theoretical model of the optical properties of sea ice in the visible and near infrared. J Geophys Res 88:9723–9735

Grenfell TC (1991) Radiative transfer model for sea ice with vertical structure variations. J Geophys Res 96:16991–17001

Grenfell TC, Hedrick D (1983) Scattering of visible and near infrared radiation by NaCl ice and glacier ice. Cold Regions Sci Technol 8:119–127

Grenfell TC, Maykut GA (1977) The optical properties of ice and snow in the Arctic Basin. J Glaciol 18:445–463

Grenfell TC, Perovich DK (1981) Radiation absorption coefficients of polycrystalline ice from 400–1400 nm. J Geophys Res 86:7447–7450 [1984 on pp. 6, 8, 17]

Grenfell TC, Warren SG, Mullen PC (1994) Reflection of solar radiation by the Antarctic snow surface at ultraviolet, visible, and near-infrared wavelengths. J Geophys Res 99:18669–18684

Gurney KR (1998) Evidence for increasing ultraviolet irradiance at Point Barrow, Alaska. Geophys Res Lett 25:903–906

Heibling EW, Villafane V, Holm-Hansen O (1994) Effects of ultraviolet radiation on Antarctic marine phytoplankton photosynthesis with particular attention to the influence of mixing. In: Weiler CS, Penhale PA (eds) Ultraviolet radiation in Antarctica: measurements and biological effects. Antarctic Res Ser 62:207–228

Jin Z, Stamnes K, Weeks WF (1994) The effect of sea ice on the solar energy budget in the atmosphere-sea ice-ocean system: a model study. J Geophys Res 99(C12):25281–25294

Karentz D (1994) Ultraviolet tolerance mechanisms in Antarctic marine organisms. In: Weiler CS, Penhale PA (eds) Ultraviolet radiation in Antarctica: measurements and biological effects. Antarct Res Ser 62:93–110

Liou KN (1974) Analytic two-stream and four-stream solutions for radiative transfer. J Atmos Sci 31:1473–1475

Maykut GA, Grenfell TC (1975) The spectral distribution of light beneath first-year sea ice in the Arctic Ocean. Limnol Oceanogr 20:554–563

Maykut GA, Light B (1995) Refractive index measurements in freezing sea ice and sodium chloride brines. Appl Optics 34:950–961

McKenzie RL, Paulin KJ, Madronich S (1998) Effects of snow cover on UV irradiance and surface albedo: a case study. J Geophys Res 103:28785–28792

Mobley CD (1994) Light and water, radiative transfer in natural waters. Academic Press, San Diego, 592 pp

Mobley CD, Cota G, Grenfell TC, Maffione RA, Pegau WS, Perovich DK (1997) Modeling light propagation in sea ice. IEEE Trans Geosci Remote Sens 36:1743–1749

Perovich DK (1990) Theoretical estimates of light reflection and transmission by spatially complex and temporally varying sea ice covers. J Geophys Res 95:9557–9567

Perovich DK (1993) A theoretical model of ultraviolet light transmission through Antarctic sea ice. J Geophys Res 98:22579–22587

Perovich DK (1995) Observations of ultraviolet light reflection and transmission by first-year sea ice. Geophys Res Lett 22:1349–1352

Perovich DK (1996) The optical properties of sea ice. CRREL Monogr 96-1, 25 pp

Perovich DK, Govoni JW (1991) Absorption coefficients of ice from 250 to 400 nm. Geophys Res Lett 18:1233–1235

Perovich DK, Grenfell TC (1981) Laboratory studies of the optical properties of young sea ice. J Glaciol 27:331–346

Perovich DK, Grenfell TC (l982) A theoretical model of radiative transfer in young sea ice. J Glaciol 28:341–357

Perovich DK, Roesler CS, Pegau WS (1998a) Variability in sea ice optical properties. J Geophys Res 103:1193–1209

Perovich DK, Barber DG, Cota G, Gow AJ, Grenfell TC, Longacre J, Maffione R, Mobley CD, Onstott RG, Pegau WS, Roesler CS (1998b) Field observations of the electromagnetic properties of first-year sea ice. IEEE Trans Geosci Remote Sens 36:1633– 1641

Perovich DK et al. (1999a) Year on ice gives climate insights. EOS Trans Am Geophys Union 80:481, 485–486

Perovich DK, Grenfell TC, Light B, Richter-Menge JA, Sturm M, Tucker WB III, Eicken H, Maykut GA, Elder B (1999b) SHEBA: snow and ice studies. Cold Regions Research and Engineering Laboratory, CD-ROM, October

Perovich DK, Grenfell TC, Light B, Hobbs PV (2001) The seasonal evolution of Arctic sea ice albedo. J Geophys Res (in press)

Prezelin BB, Boucher NP, Smith RC (1994) Marine primary production under the influence of the Antarctic ozone hole: ice colors '90. In: Weiler CS, Penhale PA (eds) Ultraviolet radiation in Antarctica: measurements and biological effects. Antarct Res Ser 62:159–186

Prezelin BB, Moline MA, Matlick HA (1998) Icecolors '93: spectral UV radiation effects on Antarctic frazil ice algae. In: Lizotte MP, Arrigo KR (eds) Antarctic sea ice: biological processes, interactions, and variability. Antarct Res Ser 73:45–83

Quakenbush T, Wendler G (1994) Ultraviolet (A) and shortwave radiation on the Juneau Icefield, Alaska. Polarforschung 62:77–82

Smith RC, Baker KS (1981) Optical properties of the clearest natural waters (200–800 nm). Appl Optics 20:177–184

Smith RC, Prezelin BB, Baker KS, Bidigare RR, Boucher NP, Coley T, Karentz D, MacIntyre S, Matlick HA, Menzies D, Ondrusek M, Wan Z, Waters KJ (1992) Ozone depletion:

ultraviolet radiation and phytoplankton biology in Antarctic waters. Science 255:952–959

Sturm M, Holmgren J, Perovich D (2001) The winter snow cover on the sea ice of the Arctic Ocean at SHEBA: temporal evolution and spatial variability. J Geophys Res (in press)

Trodahl HJ, Buckley RG (1989) Ultraviolet levels under sea ice during the Antarctic spring. Science 245:194–195

Trodahl HJ, Buckley RG (1990) Enhanced ultraviolet transmission of Antarctic sea ice during the austral spring. Geophys Res Lett 17:2177–2179

Trodahl HJ, Buckley RJ, Brown S (1987) Diffusive transport of light in sea ice. Appl Optics 26:3005–3011

Tucker WB III, Perovich DK, Gow AJ, Weeks WF, Drinkwater MR (1993) Physical properties of sea ice relevant to remote sensing. In: Carsey F (ed) The remote sensing of sea ice, chap 2. AGU Press, Washington, DC, 462 pp

Van de Hulst HC (1981) Light scattering by small particles. Dover, New York, 470 pp

Vernet M, Brody EA, Hom-Hansen O, Mitchell BG (1994) The response of Antarctic phytoplankton to ultraviolet radiation: absorption, photosynthesis, and taxonomic composition. In: Weiler CS, Penhale PA (eds) Ultraviolet radiation in Antarctica: measurements and biological effects. Antarct Res Ser 62:143–158

Warren SG (1982) Optical properties of snow. Rev Geophys Space Phys 20:67–89

Warren SG, Radinov VF, Bryazgin NN, Aleksandrov YI, Colony R (1999) Snow depth on Arctic sea ice. J Climate 12:1814–1829

Weeks WF (1998) Growth conditions and the structure and properties of sea ice. In: Lepparanta M (ed) The physics of ice-covered seas. Helsinki University Press, Helsinki, pp 25–104

Weeks WF, Ackley SF (1982) The growth, structure, and properties of sea ice. CRREL monograph 82-1. Cold Regions Research and Engineering Laboratory, Hanover, 130 pp

Wendler G, Quakenbush T (1993) Ultraviolet radiation and its extinction in Antarctic sea ice. Antarct J 84–85

Wiscombe WJ, Warren SG (1980) A model for the spectral albedo of snow. 1. Pure snow. J Atmos Sci 37(12):2712–2733

Zeebe RE, Eicken H, Robinson DH, Wolf-Gladrow D, Dieckmann GS (1996) Modeling the heating and melting rate of sea ice through light absorption by microalgae. J Geophys Res 101:1163–1181